Spontaneously excited pulses in an optically driven semiconductor laser

Sebastian Wieczorek[1,*] and Daan Lenstra[1,2]
[1]*Department of Physics and Astronomy, FEW, Vrije Universiteit, De Boelelaan 1081, 1081 HV Amsterdam, The Netherlands*
[2]*COBRA Research Institute, Eindhoven, The Netherlands*
(Received 10 April 2003; published 30 January 2004)

In optically injected semiconductor lasers, intrinsic quantum noise alone, namely, the spontaneous emission and the shot noise, are capable of exciting intensity multipulses from a steady state operation. Noisy lasers exhibit self-pulsations in the locking region of the corresponding deterministic system. The interpulse time statistics are studied in parameter regions near *k*-homoclinic (Shilnikov) bifurcations where the corresponding deterministic model exhibits single-, double-, and triple-pulse excitability. These statistics differ significantly among each other, and they could be used to characterize regions of different multipulse excitability in a real laser device.

DOI: 10.1103/PhysRevE.69.016218 PACS number(s): 82.40.Bj, 42.60.Mi, 42.65.Sf, 42.55.Px

The influence of noise on nonlinear dynamics is an important topical problem being intensively developed in mathematics [1] on the one hand and having applications in physics, chemistry [2], and biology [3] on the other hand.

This paper deals with a modern effect of noise, namely, excitability, an interdisciplinary problem [4], also recently found and studied in many laser systems [5–13]. An excitable system, after being triggered from its stable equilibrium by a small perturbation above a certain threshold, produces a large response signal before settling back to the equilibrium. This phenomenon can be associated with certain geometric realizations in phase space near saddle-node bifurcation, and very often near a homoclinic bifurcation [13]. Noise-induced excitability is related to the more general escape problem, where noise drives a system out of a potential well (corresponding to a stable equilibrium) over the potential barrier [2,14]. Here we show that the intrinsic noise associated with spontaneous recombination can excite intensity pulses in an optically injected semiconductor laser.

So far, while studying influence of noise on laser dynamics, investigators have mainly focused on semiconductor lasers subject to external optical feedback and lasers with saturable absorber. Those studies used low (two)-dimensional mathematical models where the investigators had to either choose arbitrary noise level or apply an external source of noise to obtain and study desirable effects. An activated escape approach was used to study the influence of noise on intensity dropouts in a semiconductor laser subject to external optical feedback [9,15], and the same dropout phenomenon was investigated from an excitability point of view in Ref. [8]. Externally injected noise was applied to obtain coherence resonance in a laser with saturable absorber [7]. Recently, it was claimed that spontaneous emission noise itself can be essential in organizing the above-mentioned intensity dropouts [16].

In this paper, we study noise-induced excitability in a semiconductor laser with optical injection at parameter settings near a special bifurcation point called Belyakov bifurcation [17], recently found in an injected laser system [12]. Belyakov points can appear in vector fields that are at least three dimensional. Near such a point in parameter space, there exist *k*-homoclinic bifurcation curves which bound regions of excitability [12]. At parameter settings inside those regions a single perturbation produces a deterministic *k*-pulse response ($k=1,2,3,\ldots$), an effect called multipulse excitability [12]. We will demonstrate that the intrinsic noise of the laser by itself is able to excite these multipulses, and, furthermore, we show how these regions of single-, double-, and triple-pulse excitability in a noisy laser can be distinguished on the basis of the corresponding interpulse time distributions.

The dynamics of a single-mode semiconductor laser subject to optical injection can be very well modeled by a three-dimensional system of rate equations [19] for the complex electric field $E=E_x+iE_y$ and the inversion n (number of electron-hole pairs):

$$\begin{aligned}\dot{E}_x &= K+\omega E_y+\tfrac{1}{2}(E_x-\alpha E_y)n+F_x(t),\\ \dot{E}_y &= -\omega E_x+\tfrac{1}{2}(\alpha E_x+E_y)n+F_y(t),\\ \dot{n} &= -2\Gamma n-(1+2Bn)[E_x^2+E_y^2-1]+F_n(t).\end{aligned} \tag{1}$$

Equations (1) are scaled for convenience; the connection between the scaled quantities used here and experimental quantities is given in Ref. [18].

Spontaneous emission noise as well as shot noise are modeled by a Gaussian white noise with zero mean,

$$\langle F_\kappa(t)\rangle=0 \quad (\kappa=x,y,n). \tag{2}$$

The stochastic terms satisfy:

$$\langle F_\kappa(t)F_\lambda(t')\rangle=D_{\kappa\kappa}\delta_{\kappa\lambda}(t-t') \quad (\kappa,\lambda=x,y,n), \tag{3}$$

where

$$D_{xx}=D_{yy}=R/(2\omega_R P_0); \quad D_{nn}=\omega_R J_{thr}/(J-J_{thr})^2. \tag{4}$$

*Present address: Sandia National Laboratories. Email: smwiecz@sandia.gov

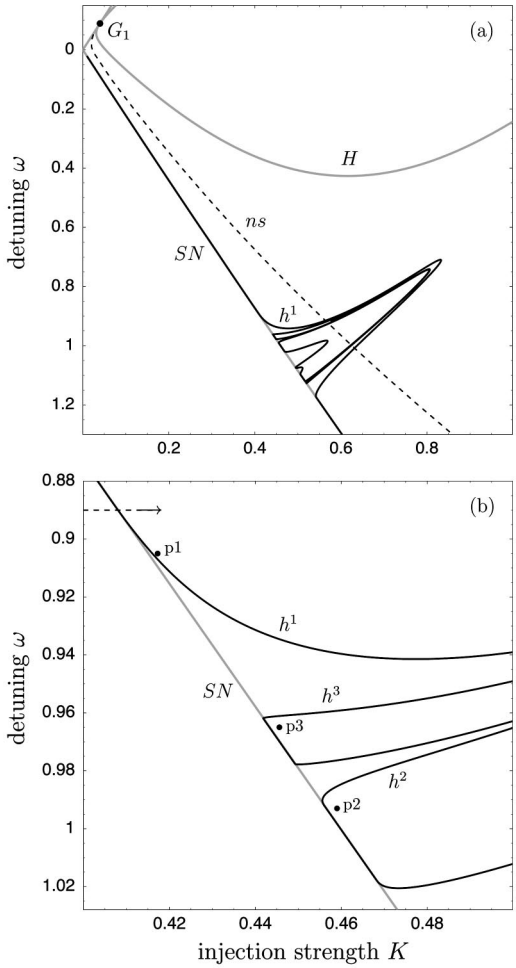

FIG. 1. The bifurcation diagram of the corresponding deterministic system in the (K,ω) plane.

Here $R=10^{12}$ s^{-1} is the spontaneous emission rate into the lasing mode, $\omega_R=2.2\times10^{10}$ rad/s and $P_0=0.75\times10^5$ are the solitary laser relaxation oscillation frequency and photon number, respectively, $J=3.6\times10^{17}$ s^{-1} is the pump rate, and $J_{thr}=3\times10^{17}$ s^{-1} is the solitary laser threshold value ($J=1.2J_{thr}$). Hence, the values for the normalized diffusion coefficients are $D_{xx}=D_{yy}=3.2\times10^{-4}$, $D_{nn}=1.8\times10^{-6}$. These values are normal for an edge-emitting laser. Equations (1) are integrated using Euler's method in DsTOOL [20].

Before we choose parameters to study the stochastic equations (1) we focus on some bifurcations of the corresponding deterministic system (i.e., when $F=0$). Figure 1(a) shows the bifurcation diagram of an injected laser in the (K,ω) parameter plane; K is the strength of the light injected into the laser and ω denotes the detuning between the frequency of the injected light and the frequency of an unperturbed (free running) laser. Stable equilibrium, corresponding to locking to the injected signal, exists for parameter settings between the lower parts of the saddle-node bifurcation curve SN and the Hopf bifurcation curve H. These two curves, shown in gray, become tangent at the codimension-two point G_1 [18]. Furthermore, there is a homoclinic bifurcation curve h^1, shown in black, of one-homoclinic orbit to saddle focus

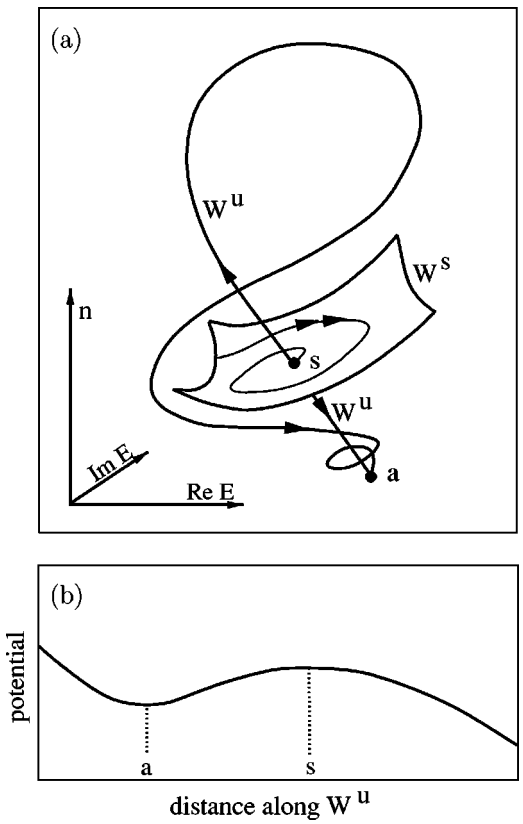

FIG. 2. Sketch of the phase portrait near (outside) h^1 tooth (a) and the potential along W^u (b).

s born along SN. The h^1 curve overlaps with SN and sometimes extends into the locking region, in a form of a *tooth*, where it intersects with the neutral saddle curve ns creating Belyakov bifurcation points. Belyakov points imply the existence of many k-homoclinic bifurcation curves, forming *tongues* in the (K,ω) plane, of which we show h^2 and h^3 in Fig. 1. More details on bifurcations near Belyakov points can be found in Ref. [12], and references therein.

Figure 2(a) shows a sketch of the phase portrait near (outside) the tooth of h^1. The two-dimensional stable manifold W^s of the saddle s forms the excitability threshold. The two branches of the unstable manifold W^u connect to the stable equilibrium a. The lower branch of W^u makes a straight connection while the upper one forms a loop before coming to a. Once the laser is perturbed from its stable equilibrium a above the threshold W^s, it produces an intensity pulse (follows the upper branch of W^u) before settling back to the stable equilibrium. Consequently, inside a $h^{k>1}$ tongue, a single perturbation above the threshold results in k intensity pulses [12]; see computed phase portraits (a1)–(a3) in Fig. 3.

The manifold W^u is the most probable escape path from the stable equilibrium. Since the parameters were chosen close to the saddle-node bifurcation SN, attraction in the two-dimensional plane parallel to W^s (near s and a) is much stronger than repulsion from s along W^u. In consequence, noisy trajectories of the laser (operating near equilibrium a) stay close to W^u during their random walk. Furthermore, the potential along W^u, sketched in Fig. 2(b), is so flat that the noise strength along W^u exceeds the deterministic force even

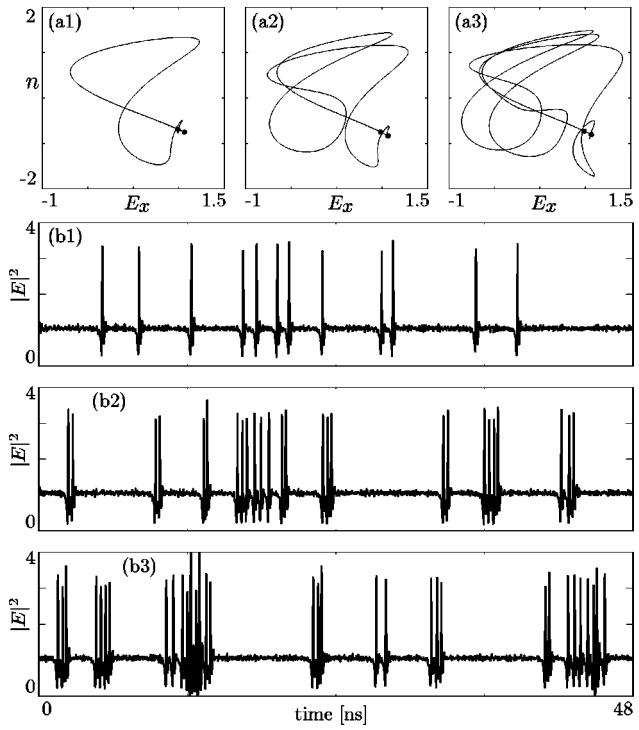

FIG. 3. Phase portraits of the deterministic system (a1)–(a3) together with the corresponding time series (b1)–(b3) featuring pulses excited by noise. From 1 to 3 (K,ω) take values: (0.417, −0.905), (0.459,−0.993), (0.4453,−0.965) as indicated by p1–p3 in Fig. 1(b).

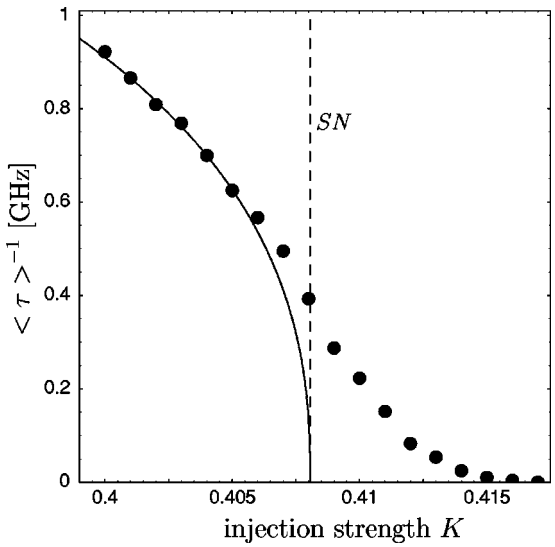

FIG. 4. The laser's pulsation frequency as the locking region, indicated by the dashed line *SN*, is approached from left to right at $\omega=-0.89$. Solid line corresponds to the deterministic system and dots correspond to the noisy laser.

away from *s* or *a*. Hence, crossing the excitability threshold (of the deterministic system) in the noisy laser does not always imply creation of pulses. Noise dominated dynamics near *s* plus the fact that our system is three dimensional make us restrict our focus to numerical investigations only.

We now demonstrate that the laser's intrinsic noise itself is able to excite pulses in an optically injected laser. To this end we fix $\omega=-0.89$, increase K across the locking border *SN* of the corresponding deterministic system, and plot in Fig. 4 the reciprocal of the interpulse time interval τ. At lower K the deterministic laser system (solid curve) oscillates at a frequency that agrees with the average τ^{-1} of the noisy laser (dots). As *SN* is approached, the oscillation period of the deterministic laser system increases exponentially to infinity. (This is characteristic for a homoclinic-saddle-node bifurcation [21] actually taking place along this part of *SN* [13].) However, for the noisy laser system τ^{-1} does not decrease to zero at *SN*. Instead, due to the noise excited pulses, the laser oscillates even within the locking region (black dots extend beyond *SN*). The further within the locking region we go, the fewer excited pulses appear and they finally disappear (for the length of time series we were able to compute) at $K\approx 0.4175$.

Next we analyze and compare distributions of time intervals between subsequent noise-induced pulses in regions of single-, double-, and triple-pulse excitability. The parameters for simulations were chosen such that in all three cases, marked by p1–p3 in Fig. 1(b), the distance between the attractor *a* and the saddle *s* is approximately the same and equals ≈ 2.1. This distance is measured along the most probable escape path, which is the lower branch of the unstable manifold W^u. In this way we compare cases with similar excitability thresholds.

In a noisy laser one can expect early triggered pulses to occur even when the laser has not yet relaxed to the attractor [8]. In case of single-pulse excitability we expect especially the ones that are launched just after the first pulse is completed but before the system has settled back to the attractor.

In the region of the phase space where the two manifolds, W^s and the upper branch of W^u, come close to each other noise has a chance to kick the trajectory from below to above the stable manifold. Once the stable manifold is crossed, the trajectory converges (parallel to the strongly attracting manifold W^s) to the upper branch of W^u, and repeats the excursion along W^u raising an early triggered pulse. This is how a pulse can be triggered before the laser has returned to the attractor. As a result, the corresponding time series consists of bursts with one or more pulses. The probability distribution from Fig. 5(a) includes the two types of events. These are the regular pulses launched from the stable equilibrium *a* and the above-discussed early triggered pulses. In our case, due to slow dynamics along W^u, the timing of early triggered pulses is spread such that they cannot be distinguished from the total distribution in Fig. 5(a); note that in some laser systems early triggered pulses may contribute to a distinct peak in the distribution [8]. The mean interpulse time for the distribution from Fig. 5(a) equals 3980 ps. This single-pulse excitability distribution is normalized to unity, while the two other distributions are normalized such that their tail areas above 2000 ps are equal in all three cases. This is to facilitate the comparison between the ratios of the number of short-spaced pulses (genuine and early triggered pulses) to the number of long-spaced pulses (first passage) for the three types of excitability.

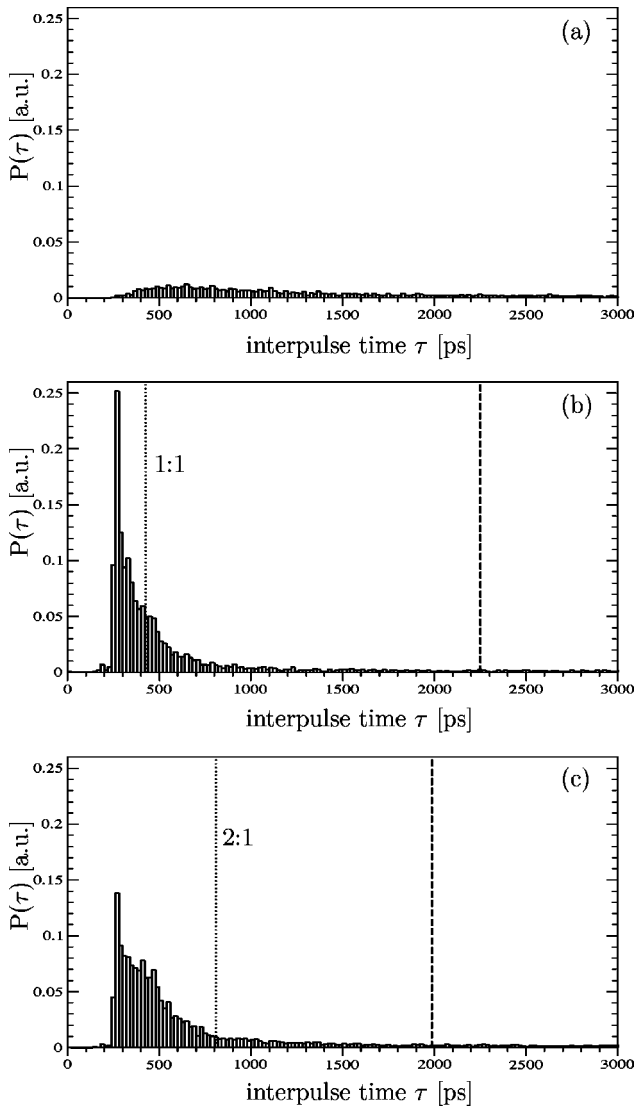

FIG. 5. Probability distributions of interpulse time τ for single- (a), double- (b), and triple-pulse (c) excitability. Corresponding parameters as in Fig. 3.

In the region of double-pulse excitability pulses are expected to appear in pairs. Indeed, the interpulse time distribution from Fig. 5(b) features a distinct peak at the time intervals near $\tau \approx 270$ ps corresponding to the intrinsic spacing between the two pulses of the genuine double pulse. The early triggered pulses are delayed when passing through the region of slow dynamics near (above) the saddle point, in contrast to the genuine double pulses created during a single quick excursion near the double loop of the upper part of W^u. These early triggered pulses show up in the distribution [Fig. 5(a)] as a shoulder of events for $\tau > 270$ ps. The dashed line denotes the mean interpulse time in the distribution (2245 ps) while the dotted line divides the distribution into two parts with the same number of events (median).

The interpulse time distribution for triple-pulse excitability [Fig. 5(c)] has two extra features not present in Fig. 5(a). The broad shoulder of events near τ between 400 ps and 500 ps corresponds to the spacing between the first and the second pulse of the genuine triple pulse. On the other hand, the pronounced peak at $\tau \approx 270$ ps corresponds to the spacing between the second and the third pulse of these triple pulses. The different appearances of the two intrinsic time spacings in the distribution is caused by noise. Actually, noise has more time to influence the longer spacing between the first and the second pulse and, hence, induces more spread in the observed timing between the first and the second pulse. Furthermore, a rather intricate structure of the triple loop [see Fig. 3(a3)] becomes affected by noise. Many bursts in the time series consist of more than three pulses and the early triggered pulses tend to be separated by intervals $\tau \approx 300$ ps contributing to the part of the distribution between the two intrinsic pulse spacings. The mean interpulse time of this distribution of 1995 ps [dashed line in Fig. 5(c)] is the shortest meaning that, on average, one burst consists of more pulses than in the two previous cases. The dotted line in Fig. 5(c) divides the distribution into two parts such that the left-hand part consists of twice as many events as the right-hand part.

We have demonstrated by theoretical analysis that quantum noise modeled by random Langevin forces can excite intensity pulses in an injected semiconductor laser. Hence, the injected laser is a self-excitable system in which the excitation is triggered from within the system and the excitability phenomenon can be studied without applying any additional perturbation.

In particular, noise substantially modifies the dynamics near the locking between the injected field and the laser field: the noisy laser can produce pulses where the deterministic model allows for locking only. This result, presented in Fig. 4, is general in the sense that it is characteristic for any forced oscillator operating near noncentral homoclinic-saddle-node bifurcation of the type studied here. We also showed how to identify regions of single-, double-, and triple-pulse excitability by highlighting different features in their interpulse time distributions. While the multipulse excitability phenomenon still remains to be experimentally confirmed, we propose the interpulse time distribution analysis as a way to detect and distinguish between different types of multipulse excitability in an experiment.

The authors would like to thank Mirvais Yousefi and Bernd Krauskopf for their helpful input.

[1] L. Arnold, *Random Dynamical Systems* (Springer-Verlag, Berlin, 1998).

[2] N.G. van Kampen, *Stochastic Processes in Physics and Chemistry* (Elsevier, Amsterdam, 1981).

[3] J.D. Murray, *Mathematical Biology* (Springer, New York, 1990).

[4] S. Grill, V.S. Zykov, and A.H. Cohen, *Excitable Oscillators as Models for Central Pattern Generators, Series on Stability,*

Vibration and Control of Systems, Series B (World Scientific, Singapore, 1997).
[5] M. Giudici, C. Green, G. Giacomelli, U. Nespolo, and J.R. Tredicce, Phys. Rev. E **55**, 6414 (1997).
[6] W. Lu, D. Yu, and R.G. Harrison, Phys. Rev. A **58**, R809 (1998).
[7] J.L.A. Dubbeldam, B. Krauskopf, and D. Lenstra, Phys. Rev. E **60**, 6580 (1999).
[8] A.M. Yacomotti, M.C. Eguia, J. Aliaga, O.E. Martinez, G.B. Mindlin, and A. Lipsich, Phys. Rev. Lett. **83**, 292 (1999).
[9] D.W. Sukow, J.R. Gardner, and D.J. Gauthier, Phys. Rev. A **56**, R3370 (1997).
[10] J.R. Tredicce, in *Nonlinear Laser Dynamics: Concepts, Mathematics, Physics, and Applications International Spring School*, edited by Bernd Krauskopf and Daan Lenstra, AIP Conf. Proc. No. 548 (AIP, Melville, NY, 2000), p. 238.
[11] H.J. Wünsche, O. Brox, M. Radziunas, and F. Henneberger, Phys. Rev. Lett. **88**, 023901 (2002).
[12] S. Wieczorek, B. Krauskopf, and D. Lenstra, Phys. Rev. Lett. **88**, 063901 (2002).
[13] B. Krauskopf, K. Schneider, J. Sieber, S. Wieczorek, and M. Wolfrum, Opt. Commun. **215**, 367 (2003).
[14] P. Hanggi, P. Talkner, and M. Borkovec, Rev. Mod. Phys. **62**, 251 (1990).
[15] J. Hales, A. Zhukov, R. Roy, and M.I. Dykman, Phys. Rev. Lett. **85**, 78 (2000).
[16] Wing-Shun Lam, Parvez N. Guzdar, and Rajarshi Roy, Int. J. Mod. Phys. B **17**, 4123 (2003).
[17] L. Belyakov, Math. Z. **36**, 838 (1984).
[18] S. Wieczorek, B. Krauskopf, and D. Lenstra, Opt. Commun. **4172**, 279 (1999).
[19] S. Wieczorek, T.B. Simpson, B. Krauskopf, and D. Lenstra, Phys. Rev. E **65**, 045207(R) (2002).
[20] A. Back, J. Guckenheimer, M.R. Myers, F.J. Wicklin, and P.A. Worfolk, Not. Am. Math. Soc. **39**, 303 (1992).
[21] Yu.A. Kuznetsov, *Elements of Applied Bifurcation Theory* (Springer, New York, 1995).